J Syst Sci Complex (2018) 31: 1103–1127

Low-Dimensional SIR Epidemic Models with Demographics on Heterogeneous Networks*

JING Wenjun · JIN Zhen · ZHANG Juping

DOI: 10.1007/s11424-018-7029-8
Received: 10 February 2017 / Revised: 5 May 2017

Abstract To investigate the impacts of demographics on the spread of infectious diseases, a susceptible-infectious-recovered (SIR) pairwise model on heterogeneous networks is established. This model is reduced by using the probability generating function and moment closure approximations. The basic reproduction number of the low-dimensional model is derived to rely on the recruitment and death rate, the first and second moments of newcomers' degree distribution. Sensitivity analysis for the basic reproduction number is performed, which indicates that a larger variance of newcomers' degrees can lead to an epidemic outbreak with a smaller transmission rate, and contribute to a slight decrease of the final density of infectious nodes with a larger transmission rate. Besides, stochastic simulations indicate that the low-dimensional model based on the log-normal moment closure assumption can well capture important properties of an epidemic. And the authors discover that a larger recruitment rate can inhibit the spread of disease.

Keywords Complex networks, demographic process, moment closure approximation, probability generating function.

1 Introduction

Mathematical models play an important role in understanding the spread and control of infectious diseases, among which well-mixed models[1–5] and network-based models[6–18] have been widely studied. From the perspective of network topological structure, the former is essentially based on homogeneous networks in which each individual has the same probability to contact others, while the latter is based on heterogeneous networks in which contacts between individuals are heterogeneous. The well-mixed models allow one to easily incorporate many factors such as the demographic effects into epidemic models, but it ignores the heterogeneity of contacts between individuals. Networks are introduced as an attempt to make up for

JING Wenjun · JIN Zhen · ZHANG Juping
Complex Systems Research Center, Shanxi University, Taiyuan 030006*, China.* Email: jinzhn@263.net.
*This research was supported by the National Natural Science Foundation of China under Grant Nos. 11331009, 11471197, 11501340, and 11601294, as well as the Youth Science Fund of Shanxi Province under Grant No. 2015021020.
◇ *This paper was recommended for publication by Editor DI Zengru.*

this deficiency by denoting nodes as individuals and edges as contacts between individuals. Such network-based models give a better understanding of the role of contact heterogeneity in epidemic spreading, and thus receive significant attention from researchers.

Current studies about epidemic models on networks mostly focus on static networks. Many interesting results have been obtained in this area[6, 8, 11–13]. Particularly, Pastor-Satorras and Vespignani[6] found that there is no epidemic threshold in scale-free networks following a power-law degree distribution $p(k) \propto k^{-\gamma}$ with exponents $2 < \gamma \leqslant 3$. However, the demographic process of individuals are not considered in these models. In fact, for a long-course epidemic, such as hepatitis, individuals' contact pattern varies on a time scale comparable to that of the epidemic spreading process. Specifically, newborn individuals join the network and dead individuals leave the network during an epidemic. These demographic dynamics have a significant effect on the network structure which in turn affects the epidemic spreading. Since this complex interplay raises great challenges for mathematical modelling and analysis, research on this topic has been scare, except for a few notable examples. By using the probability generating function, Kamp proposed an SID model and an SI_1I_2D model of HIV epidemics to investigate the interplay between epidemic spreading and network dynamics[19, 20]. Jin, et al.[21] established an SIS epidemic model with demographics and analyzed the stability of the model. Moreover, Piccardi, et al.[22] investigated the effects of birth and death processes on the network structure and the spread of epidemics. They found that the most likely to be infected nodes are those with intermediate degrees for the SIR process in most networks, but the ERN (Erdős-Rényi network[23]) case is an exception. Unlike the above models, we will investigate the effects of demographics on epidemic spreading by the pairwise model.

Pairwise models have been a popular approach to study the dynamics on networks[10, 24–27]. Considering the fact that the disease can be transmitted only when a susceptible individual contacts with an infectious one, pairwise models track how the number of such contacts varies with time. The number of pairs depends further on the number of triples, making the model analytically intractable. To close the pairwise models, the number of pairs and triples are estimated by numerous moment closure methods, such as the deconvolution of individuals[10] and the triple closure[25]. Pairwise models have been successfully used in static networks, but there has been no work in studying the epidemic dynamics with demographics, inspiring our investigation. A pairwise model with demographics on heterogeneous networks is established. It is a high dimensional model and takes huge difficulties for mathematical analysis in theory. In order to obtain a low-dimensional model, the pairwise model is expressed with another form depending on the moments of the susceptible degree distribution. However, the equation for a given moment is coupled to the equations of higher order moments, leading to an infinite but countable number of equations. To truncate the model at a low dimension, the log-normal moment closure assumption in [28, 29] is used. With the low-dimensional model, the effects of demographics on the network structure and epidemic spreading are investigated.

The remainder of this paper is organized as follows: Section 2 proposes the SIR epidemic model with demographics on heterogeneous networks. The basic reproduction number of the model and its relationship with recruitment rate are derived in Section 3. Stochastic and

numerical simulations are performed to verify the analytical results in Section 4. Finally, Section 5 presents the major conclusions of this paper.

2 SIR Epidemic Models with Demographics on Heterogeneous Networks

2.1 Pairwise Model

A pairwise SIR epidemic model with demographics on heterogeneous networks is established in this section. We model the population as a time-varying network with $N(t)$ nodes (i.e., individuals). The links connecting nodes represent the contacts between individuals. The number of links one node has is defined as the degree of this node. Each node can be in one of the three states: Susceptible S, infectious I, and recovered R. For $A, B, C \in \{S, I, R\}$, we set $[A_k]$ to be the expected number of nodes with degree k in the network, $[A_k B_l]$ to be the expected number of $A_k - B_l$ pairs in the network, i.e., the number of links from nodes in state A with degree k to nodes in state B with degree l, $[A_k B_l C_m]$ to be the expected number of $A_k - B_l - C_m$ triples in the network, i.e., the number of relationships for which the central node has state B with degree l and the other two neighboring nodes have state A with degree k and state C with degree m, respectively. When there is no subscript, it represents the sum of all possible degrees, such as $[A_k B] = \sum_l [A_k B_l]$ and $[AB] = \sum_k [A_k B]$. This counting method indicates that pairs are counted once in each direction such that $[AB] = [BA]$ and that $[AA]$ is even. Similarly, $[ABA]$ is even. More notations used are summarized in Table 1.

During the epidemic spreading over a network, a susceptible node can be infected by its neighboring infectious nodes with a per link transmission rate λ, and infectious nodes recover to full immunity at a rate γ. In addition, each node, together with its links, departs from the network due to death with a rate d. Meanwhile, each node gives birth to another node at a rate b, irrespective of its epidemic state. A new node randomly establishes k contacts to existing nodes with probability π_k, whose probability generating function is $\psi(x) = \sum_k \pi_k x^k$. New nodes are immunized with probability p, thus they are recovered with probability p or susceptible with probability $1 - p$. We then consider the variation of nodes in each class in a short time interval Δt from the following four independent processes:

Infection Susceptible nodes are infected by their infectious neighbors, resulting in $\lambda[S_k I]\Delta t$ susceptible nodes of degree k becoming infectious nodes of degree k.

Recovery Each infectious node recovers and enters the recovered class with probability $\gamma\Delta t$, resulting in $\gamma[I_k]\Delta t$ infectious nodes of degree k becoming recovered nodes of degree k.

Death process The death of nodes causes a loss of nodes in A_k by $d[A_k]\Delta t$. Meanwhile, the removal of links alters the degree of the connecting nodes, resulting in $dk[A_k]\Delta t$ nodes in A_k becoming nodes in A_{k-1}.

Recruitment process The total number of newcomers in a short time interval Δt is $bN\Delta t$. Because newcomers are immunized with probability p and have degree k with probability π_k, the number of newly susceptible and recovered nodes of degree k is $(1-p)bN\pi_k\Delta t$ and $pbN\pi_k\Delta t$, respectively. Besides, the degree of a node in A_k will change from k to $k+1$ when a newcomer

attaches to it. Since the average degree of newcomers is $\psi'(1)$, the total number of links introduced by newcomers is $bN\psi'(1)\Delta t$. These new links contact existing nodes randomly, leading to $b\psi'(1)[A_k]\Delta t$ nodes in A_k entering the class A_{k+1}.

Table 1 Notations and parameters of the model

b	recruitment rate
d	death rate
p	immunization rate
λ	transmission rate per $S-I$ link
γ	cure rate
π_k	probability that a newcomer has k contacts
N	total number of nodes in the network
$[A_k]$	the number of nodes in state A with degree k
$[A]=\sum_k[A_k]$	total number of nodes in state A
$[AB]$	the number of pairs with one node in state A and the other node in state B
$[AA]$	double the number of unique $A-A$ links
$[ABC]$	the number of $A-B-C$ triple in the network
$[ABA]$	double the number of unique $A-B-A$ triples
$[A_kB]\approx p_{ab}k[A_k]$	the number of links with one node in state A with degree k and the other node in state B
$[A_k\cdot]=k[A_k]$	the number of links emanating from nodes in state A with degree k
$[A\cdot]=\sum_k k[A_k]$	the number of links emanating from nodes in state A
$p_k=\frac{N_k}{N}$	probability that a randomly selected node has a degree k
$p_{ab}=\frac{[AB]}{\sum_k k[A_k]}$	probability that a link starting from a node in state A to point to a node in state B
$p_{a_k}=\frac{[A_k]}{[A]}$	probability that a node in state A has degree k
$g_a(x,t)=\sum_k p_{a_k}x^k$	probability generating function of p_{a_k}
$g(x,t)=\sum_k p_kx^k$	probability generating function of p_k
$\psi(x)=\sum_k \pi_kx^k$	probability generating function of π_k
$\psi'(1)=\frac{\partial\psi(x)}{\partial x}\big\vert_{x=1}$	the average degree of newcomers
$\psi''(1)=\frac{\partial^2\psi(x)}{\partial^2 x}\big\vert_{x=1}$	
$\psi^{(m)}(1)=\frac{\partial^m\psi(x)}{\partial^m x}\big\vert_{x=1}$	

To give an intuitive representation of the above processes, a flow diagram of this model is shown in Figure 1.

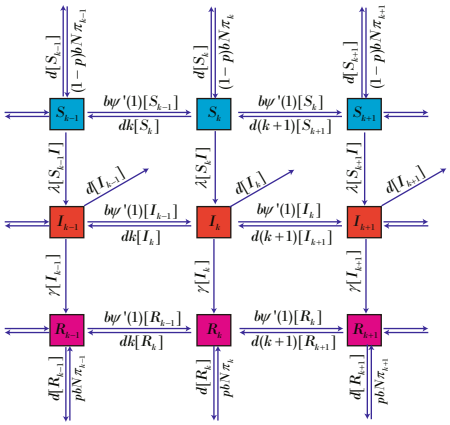

Figure 1 Flow diagram of transmission dynamics for the number of nodes in different state and degree

According to Figure 1, the SIR epidemic model is given by the following equations:

$$\begin{aligned}[\dot{S}_k] =&(1-p)bN\pi_k - \lambda[S_kI] - d[S_k] + bN\psi'(1)\left(\frac{[S_{k-1}]}{N} - \frac{[S_k]}{N}\right)\\ &- d\left(k[S_k] - (k+1)[S_{k+1}]\right), \end{aligned} \tag{1}$$

$$[\dot{I}_k] =\lambda[S_kI] - (d+\gamma)[I_k] + bN\psi'(1)\left(\frac{[I_{k-1}]}{N} - \frac{[I_k]}{N}\right) - d(k[I_k] - (k+1)[I_{k+1}]), \tag{2}$$

$$[\dot{R}_k] =pbN\pi_k - d[R_k] + \gamma[I_k] + bN\psi'(1)\left(\frac{[R_{k-1}]}{N} - \frac{[R_k]}{N}\right) - d(k[R_k] - (k+1)[R_{k+1}]). \tag{3}$$

Assuming that given a node in state A with degree k, the state of connected node is independent of k and therefore independent of the local structure[10], it has

$$[A_kB] \approx [AB]\frac{k[A_k]}{\sum_m m[A_m]}. \tag{4}$$

Then Equations (1)–(3) become

$$\begin{aligned}[\dot{S}_k] =&(1-p)bN\pi_k - \lambda[SI]\frac{k[S_k]}{\sum_m m[S_m]} - d[S_k] + b\psi'(1)([S_{k-1}] - [S_k])\\ &- d(k[S_k] - (k+1)[S_{k+1}]), \end{aligned} \tag{5}$$

$$[\dot{I}_k] =\lambda[SI]\frac{k[S_k]}{\sum_m m[S_m]} - (d+\gamma)[I_k] + b\psi'(1)([I_{k-1}] - [I_k]) - d(k[I_k] - (k+1)[I_{k+1}]), \tag{6}$$

$$[\dot{R}_k] =pbN\pi_k - d[R_k] + \gamma[I_k] + b\psi'(1)([R_{k-1}] - [R_k]) - d(k[R_k] - (k+1)[R_{k+1}]). \tag{7}$$

Obviously, these equations are not closed since $[SI]$ is an unknown quantity. Similar to [10], the dynamical equation for $[SI]$ is derived by

$$[\dot{S}I] = -\lambda[SI] - \lambda[ISI] + \lambda[SSI] - \gamma[SI] - 2d[SI] + (1-p)b\psi'(1)[I]. \tag{8}$$

In Equation (8), the first term indicates that a susceptible node in the $S-I$ pair is infected by its infectious neighbor within the pair, while the second term indicates that it is infected by infectious neighbors outside the pair. Similar to the second term, the third term means that an $S-S$ pair turns into an $S-I$ pair due to the infection of S by one of their infectious neighbors outside this $S-S$ pair. The forth term represents that the infectious node in the $S-I$ pair recovers. The term $-2d[SI]$ indicates that one of the nodes in the $S-I$ pair dies, leading to the disappearance of $S-I$ pair. For the last term, the total number of newcomers in one time step Δt is $bN\Delta t$. Because each of them has an average degree of $\psi'(1)$ and takes a vaccination with probability p, the total number of edges starting from susceptible newcomers is $(1-p)bN\psi'(1)\Delta t$. Since newcomers link to existing nodes randomly, the number of newly formed $S-I$ pairs is $(1-p)b\psi'(1)[I]\Delta t$.

Note that the number of nodes depends on the number of pairs, and the number of pairs depends on the number of triples. In this manner, the model is closed only when it reaches the network size if we continue to write higher-order equations for triples and so on. In order to obtain a low-dimensional model, we need the approximations of $[SSI]$ and $[ISI]$ triples in terms of the number of pairs and nodes. Intuitively, assuming that the number of $A-S_k-I$ triples can be counted by considering all $(k-1)[AS_k]$ stubs emanating from S_k nodes which are already connected to a node in state A and multiplying the probability that such stubs will connect to an infectious node (i.e., $\frac{[S_kI]}{k[S_k]}$). Following [25], the triple closure is given by

$$[AS_kI] \approx (k-1)[AS_k]\frac{[S_kI]}{k[S_k]}.$$

Furthermore, one has

$$[ASI] = \sum_k [AS_kI] \approx \sum_k (k-1)[AS_k]\frac{[S_kI]}{k[S_k]}. \tag{9}$$

This closure is under the assumption that the number of susceptible neighbors of a susceptible node with degree k is binomially distributed, that is, knowing that one neighbor is susceptible tells us nothing about the status of another neighbor[30]. Combining this assumption with Equation (4) yields

$$[SSI] \approx [SS][SI]\frac{\sum_k (k-1)k[S_k]}{(\sum_m m[S_m])^2}, \tag{10}$$

$$[ISI] \approx [SI]^2\frac{\sum_k (k-1)k[S_k]}{(\sum_m m[S_m])^2}. \tag{11}$$

Furthermore, the dynamical equation for $[SS]$ is obtained by the following equation

$$[\dot{SS}] = 2(1-p)b\psi'(1)[S] - 2\lambda[SSI] - 2d[SS]. \tag{12}$$

Thus, substituting Equations (10) and (11) into Equations (5)–(8) and (12) leads to the following

closed pairwise model

$$\begin{cases} [\dot{S}_k] = (1-p)bN\pi_k - \lambda[SI]\dfrac{k[S_k]}{\sum_m m[S_m]} - d[S_k] + b\psi'(1)([S_{k-1}]-[S_k]) \\ \qquad -d(k[S_k]-(k+1)[S_{k+1}]), \\ [\dot{I}_k] = \lambda[SI]\dfrac{k[S_k]}{\sum_m m[S_m]} - (d+\gamma)[I_k] + b\psi'(1)([I_{k-1}]-[I_k]) - d(k[I_k]-(k+1)[I_{k+1}]), \\ [\dot{R}_k] = pbN\pi_k - d[R_k] + \gamma[I_k] + b\psi'(1)([R_{k-1}]-[R_k]) - d(k[R_k]-(k+1)[R_{k+1}]), \\ [\dot{SI}] = -\lambda[SI] - \lambda[SI]^2\dfrac{\sum_l (l-1)l[S_l]}{(\sum_m m[S_m])^2} + \lambda[SS][SI]\dfrac{\sum_l (l-1)l[S_l]}{(\sum_m m[S_m])^2} \\ \qquad -2d[SI] - \gamma[SI] + (1-p)b\psi'(1)[I], \\ [\dot{SS}] = 2(1-p)b\psi'(1)[S] - 2\lambda[SS][SI]\dfrac{\sum_l (l-1)l[S_l]}{(\sum_m m[S_m])^2} - 2d[SS]. \end{cases} \tag{13}$$

However, the dimension of Model (13) is high, and even infinity if the degree of node follows a power-low distribution. This motivates us to reduce the model size.

2.2 A High-Dimensional Model Based on the Probability Generating Function

In this section, we will use the probability generating function to express Model (13). Similar to [19, 20], we introduce the probability that an edge emanating from a susceptible node points to an infectious node, i.e.,

$$p_{si} = \frac{[SI]}{\sum_m m[S_m]}. \tag{14}$$

Moreover, let the degree distribution of susceptible nodes at time t be

$$p_{s_k}(t) = \frac{[S_k](t)}{[S](t)}, \quad k = 1, 2, \cdots.$$

The probability generating function of $p_{s_k}(t)$ is denoted as $g_s(x,t)$ with the form

$$g_s(x,t) = \sum_k p_{s_k}(t)x^k, \tag{15}$$

where x is a dummy variable. For convenience, we denote the partial derivative with respect to time and the dummy variable by a dot and a prime, respectively, through out this paper. That is,

$$\dot{g}_s(x,t) = \frac{\partial g_s(x,t)}{\partial t}, \quad g'_s(x,t) = \frac{\partial g_s(x,t)}{\partial x}, \quad g_s^{(m)}(x,t) = \frac{\partial^m g_s(x,t)}{\partial x^m},$$

where $g_s^{(m)}(x,t)$ denotes the mth partial derivative with respect to the dummy variable. Thus, $g'_s(1,t) = \frac{\partial g_s(x,t)}{\partial x}|_{x=1}$ is the average degree of susceptible nodes at time t.

Focusing on the dynamical process of the total number of nodes in each state, we sum Equations (5)–(7) for all k respectively and obtain

$$[\dot{S}] = (1-p)bN - \lambda p_{si}[S]g_s'(1,t) - d[S], \tag{16}$$

$$[\dot{I}] = \lambda p_{si}[S]g_s'(1,t) - (d+\gamma)[I], \tag{17}$$

$$[\dot{R}] = pbN - d[R] + \gamma[I]. \tag{18}$$

A flow diagram of the total number of nodes in each state is shown in Figure 2. To close Equations (16)–(18), it is necessary to derive the dynamical equation for p_{si} and $g_s(x,t)$.

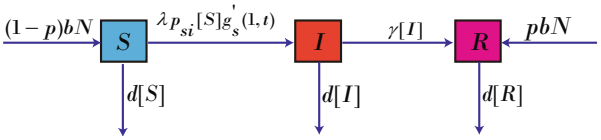

Figure 2 Flow diagram of the transmission dynamics for the total number of nodes in different state

It follows from the definition of p_{si} that

$$\dot{p}_{si} = \frac{[\dot{S}I]}{[S\cdot]} - \frac{[\dot{S}\cdot]}{[S\cdot]}p_{si}. \tag{19}$$

On the other hand, equation for $[\dot{S}I]$ in Model (13) can be rewritten as

$$[\dot{S}I] = -\lambda[SI]\left(p_{si}\frac{g_s''(1,t)}{g_s'(1,t)} - p_{ss}\frac{g_s''(1,t)}{g_s'(1,t)}\right) - (\lambda+2d+\gamma)[SI] + (1-p)b\psi'(1)[I]. \tag{20}$$

Multiplying Equation (5) by k and summing up over k, one obtains

$$[\dot{S}\cdot] = b\psi'(1)((1-p)N + [S]) - \lambda p_{si}[S](g_s''(1,t) + g_s'(1,t)) - 2d[S\cdot]. \tag{21}$$

Substituting Equations (20)–(21) into Equation (19) yields

$$\begin{aligned}\dot{p}_{si} =& \lambda p_{si}p_{ss}\frac{g_s''(1,t)}{g_s'(1,t)} - (\lambda+\gamma-\lambda p_{si})p_{si} \\ &+ \frac{b\psi'(1)}{[S]g_s'(1,t)}\left[(1-p)[I] - ((1-p)N + [S])p_{si}\right].\end{aligned} \tag{22}$$

Note that equation of $\dot{p}_{si}$ contains another variable p_{ss}. Similar to the derivation of $\dot{p}_{si}$, the dynamical equation for p_{ss} can be derived as

$$\dot{p}_{ss} = -\lambda p_{si}p_{ss}\frac{g_s''(1,t)}{g_s'(1,t)} + \lambda p_{si}p_{ss} + \frac{b\psi'(1)}{[S]g_s'(1,t)}\left(2(1-p)[S] - ((1-p)N + [S])p_{ss}\right). \tag{23}$$

Now we derive the dynamical equation for $g_s(x,t)$. It follows from (15) that

$$\dot{g}_s(x,t) = \sum_k \left(\frac{[\dot{S}_k]}{[S]} - \frac{\dot{S}}{[S]}p_{s_k}\right)x^k. \tag{24}$$

Inserting Equations (5) and (16) into Equation (24) yields

$$\begin{aligned}\dot{g}_s(x,t) =&(1-p)b\frac{N}{S}(\psi(x)-g_s(x,t))-\lambda p_{si}(xg_s'(x,t)-g_s'(1,t)g_s(x,t))\\&-b(1-x)\psi'(1)g_s(x,t)+d(1-x)g_s'(x,t).\end{aligned}\tag{25}$$

As the derivatives of $g_s(x,t)$ only for $x=1$ are needed in $\dot{p}_{si}$ and $\dot{p}_{ss}$, the partial equation (25) can be reduced to a set of ordinary differential equations. This means that $\dot{g}_s^{(m)}(1,t)$, the mth partial derivative of $\dot{g}_s(x,t)$ with respect to x at $x=1$, is needed, where

$$\dot{g}_s^{(m)}(1,t)=\sum_k k(k-1)\cdots(k-m+1)\left(\frac{[\dot{S}_k]}{[S]}-\frac{[\dot{S}]}{[S]}p_{s_k}\right).\tag{26}$$

Applying Equations (5) and (16) into Equation (26) results in

$$\begin{aligned}\dot{g}_s^{(m)}(1,t) =&-\lambda p_{si}\left(g_s^{(m+1)}(1,t)+mg_s^{(m)}(1,t)-g_s'(1,t)g_s^{(m)}(1,t)\right)\\&+mb\psi'(1)g_s^{(m-1)}(1,t)-mdg_s^{(m)}(1,t)+(1-p)b\frac{N}{[S]}\left(\psi^{(m)}(1)-g_s^{(m)}(1,t)\right).\end{aligned}\tag{27}$$

Then differential equations (16)–(18), (22), (23) and (27) compose a closed model as follows

$$\begin{cases}[\dot{S}]=(1-p)bN-\lambda p_{si}[S]g_s'(1,t)-d[S],\\ [\dot{I}]=\lambda p_{si}[S]g_s'(1,t)-(d+\gamma)[I],\\ [\dot{R}]=pbN-d[R]+\gamma[I],\\ \dot{p}_{si}=\lambda p_{si}p_{ss}\dfrac{g_s''(1,t)}{g_s'(1,t)}-(\lambda+\gamma-\lambda p_{si})p_{si}+\dfrac{b\psi'(1)}{[S]g_s'(1,t)}\left[(1-p)[I]-((1-p)N+[S])p_{si}\right],\\ \dot{p}_{ss}=-\lambda p_{si}p_{ss}\dfrac{g_s''(1,t)}{g_s'(1,t)}+\lambda p_{si}p_{ss}+\dfrac{b\psi'(1)}{[S]g_s'(1,t)}\left[2(1-p)[S]-((1-p)N+[S])p_{ss}\right],\\ \dot{g}_s^{(m)}(1,t)=-\lambda p_{si}\left(g_s^{(m+1)}(1,t)+mg_s^{(m)}(1,t)-g_s'(1,t)g_s^{(m)}(1,t)\right)\\ \qquad\qquad +mb\psi'(1)g_s^{(m-1)}(1,t)-mdg_s^{(m)}(1,t)\\ \qquad\qquad +(1-p)b\dfrac{N}{[S]}\left(\psi^{(m)}-g_s^{(m)}(1,t)\right).\end{cases}\tag{28}$$

It is observed from Model (28) that the evolution of $g_s^{(m)}(1,t)$ depends on $g_s^{(m+1)}(1,t)$, forming an infinite number of differential equations. Hence, it is intractable to obtain the precise solutions. To solve this problem, the log-normal moment closure assumption will be used to truncate this model at a low dimension.

2.3 Reduction of Model (28) Based on Moment Closure Assumption

To reduce the dimension of Model (28), we use the moment closure assumptions which are frequently used to estimate the high order moments of a probability distribution in terms of its lower order moments based on some distributions[28, 29, 31–34]. One simple assumption is

to set the second central moment as zero (namely, zero variance assumption), then the model can be closed at the level of $g'_s(1,t)$. One advantage of this assumption is that a positive equilibrium of the model can be derived. But this assumption can not capture the variation of the variable. To get a more accurate estimation, one can specify an appropriate distribution for the variable, and then estimate the third moment by the first and second moments based on this distribution. Among these assumptions, Poisson distribution and normal distribution are commonly used. However, as mentioned in [33], all cumulants of a Poisson random variable are equal to the mean value[28, 34], and normal moment assumption can not characterize highly skewed probability distribution[35]. Thus truncation of high order moments based on these two distributions may lead to non-valid or undesirable values. In addition to Poisson and normal distributions, many other approximate distributions have been suggested, such as the log-normal distribution[28, 29]. As the log-normal distribution has nonnegative support and nonzero skewness, which are important properties in the context of nonlinear epidemic models, we will use it to reduce the dimension of Model (28). Next we give the models based on two special moment closure assumptions: The zero variance assumption and log-normal moment closure assumption.

Firstly, substituting $m = 1$ and $m = 2$ into Equation (27) respectively yields

$$\begin{aligned}\dot{g}'_s(1,t) =&(1-p)b\frac{N}{[S]}(\psi'(1) - g'_s(1,t))\\ &- \lambda p_{si}(g''_s(1,t) + g'_s(1,t) - g'_s(1,t)^2) + b\psi'(1) - dg'_s(1,t)\end{aligned} \tag{29}$$

and

$$\begin{aligned}\dot{g}''_s(1,t) =& -\lambda p_{si}(g^{(3)}_s(1,t) + 2g''_s(1,t)) + (1-p)b\frac{N}{[S]}(\psi''(1) - g''_s(1,t))\\ &+ 2b\psi'(1)g'_s(1,t) - 2dg''_s(1,t) + \lambda p_{si}g'_s(1,t)g''_s(1,t).\end{aligned} \tag{30}$$

Then we are able to close these equations if $g^{(3)}_s(1,t)$ can be expressed in terms of $g'_s(1,t)$ and $g''_s(1,t)$ or the third moment of p_{s_k} can be approximated by its first two moments.

Case 1: Log-normal moment closure assumption (LNMCA)

Ekanayake and Allen[29] assumed that when the quasi-stationary distribution of variable X is approximately log-normal, then

$$E(X^j) = \begin{cases} \left(\dfrac{E(X^{m+1})}{E(X^m)}\right)^{2m+1}, & j = 2m+1,\\ \\ \left(\dfrac{E(X^{m+1})}{E(X^{m-1})}\right)^{m}, & j = 2m,\end{cases} \tag{31}$$

where $E(X^m)$ is the mth moment of X. Specially, when $m = 1$, it has

$$E(X^3) = \left(\frac{E(X^2)}{E(X)}\right)^3. \tag{32}$$

Let $g_x(z)$ be the probability generating function of the random variable X, then

$$g_x^{(3)}(1) = E(X^3) - 3E(X^2) + 2E(X). \tag{33}$$

Combining Equations (32)–(33) gets

$$g_x^{(3)}(1) = \left(\frac{E(X^2)}{E(X)}\right)^3 - 3E(X^2) + 2E(X). \tag{34}$$

Here, it follows from Equation (34) that

$$g_s^{(3)}(1,t) = \left(\frac{g_s''(1,t) + g_s'(1,t)}{g_s'(1,t)}\right)^3 - 3g_s''(1,t) - g_s'(1,t). \tag{35}$$

Inserting it into Equation (30) yields

$$\begin{aligned}\dot{g}_s''(1,t) =& -\lambda p_{si}\left(\left(\frac{g_s''(1,t) + g_s'(1,t)}{g_s'(1,t)}\right)^3 - g_s''(1,t) - g_s'(1,t)\right)\\ &+ (1-p)b\frac{N}{[S]}(\psi''(1) - g_s''(1,t)) + 2b\psi'(1)g_s'(1,t)\\ &- 2dg_s''(1,t) + \lambda p_{si}g_s'(1,t)g_s''(1,t).\end{aligned} \tag{36}$$

Thus, Equations (16)–(18), (22), (23), (29), and (36) compose a closed epidemic model

$$\begin{cases}
[\dot{S}] = (1-p)bN - \lambda p_{si}[S]g_s'(1,t) - d[S], & \text{(37a)}\\
[\dot{I}] = \lambda p_{si}[S]g_s'(1,t) - (d+\gamma)[I], & \text{(37b)}\\
[\dot{R}] = pbN - d[R] + \gamma[I], & \text{(37c)}\\
\dot{p}_{si} = \lambda p_{si}p_{ss}\dfrac{g_s''(1,t)}{g_s'(1,t)} - (\lambda + \gamma - \lambda p_{si})p_{si} + \dfrac{b\psi'(1)}{[S]g_s'(1,t)}((1-p)I - ((1-p)N + [S])p_{si}), & \text{(37d)}\\
\dot{p}_{ss} = -\lambda p_{si}p_{ss}\dfrac{g_s''(1,t)}{g_s'(1,t)} + \lambda p_{si}p_{ss} + \dfrac{b\psi'(1)}{[S]g_s'(1,t)}\left(2(1-p)[S] - ((1-p)N + [S])p_{ss}\right), & \text{(37e)}\\
\dot{g}_s'(1,t) = (1-p)b\dfrac{N}{[S]}(\psi'(1) - g_s'(1,t)) - \lambda p_{si}(g_s''(1,t) + g_s'(1,t) - g_s'(1,t)^2)\\
\qquad\qquad +b\psi'(1) - dg_s'(1,t), & \text{(37f)}\\
\dot{g}_s''(1,t) = -\lambda p_{si}\left(\left(\dfrac{g_s''(1,t) + g_s'(1,t)}{g_s'(1,t)}\right)^3 - g_s''(1,t) - g_s'(1,t)\right) + (1-p)b\dfrac{N}{[S]}(\psi''(1) - g_s''(1,t))\\
\qquad\qquad +2b\psi'(1)g_s'(1,t) - 2dg_s''(1,t) + \lambda p_{si}g_s'(1,t)g_s''(1,t). & \text{(37g)}
\end{cases}$$

Case 2: Zero variance assumption $E(X^2) = (E(X))^2$

The variance of X being zero leads to $E(X^2) = (E(X))^2$. Furthermore, $g_s''(1,t) = g_s(1,t)^2 - g_s(1,t)$. Therefore, Model (28) is reduced to

$$\begin{cases} [\dot{S}] = (1-p)bN - \lambda p_{si}[S]g_s'(1,t) - d[S], & (38a)\\ [\dot{I}] = \lambda p_{si}[S]g_s'(1,t) - (d+\gamma)[I], & (38b)\\ [\dot{R}] = pbN - d[R] + \gamma[I], & (38c)\\ \dot{p}_{si} = \lambda p_{si}p_{ss}\dfrac{(g_s'(1,t))^2 - g_s'(1,t)}{g_s'(1,t)} - (\lambda+\gamma-\lambda p_{si})p_{si} \\ \qquad + \dfrac{b\psi'(1)}{[S]g_s'(1,t)}((1-p)[I] - ((1-p)N + [S])p_{si}), & (38d)\\ \dot{p}_{ss} = -\lambda p_{si}p_{ss}\dfrac{(g_s'(1,t))^2 - g_s'(1,t)}{g_s'(1,t)} + \lambda p_{si}p_{ss} \\ \qquad + \dfrac{b\psi'(1)}{[S]g_s'(1,t)}\left(2(1-p)[S] - ((1-p)N + [S])p_{ss}\right), & (38e)\\ \dot{g}_s'(1,t) = (1-p)b\dfrac{N}{[S]}(\psi'(1) - g_s'(1,t)) + b\psi'(1) - dg_s'(1,t). & (38f) \end{cases}$$

Compared with Model (38), it is easy to observe that Model (37) has one more equation. It can capture the effects of variance of newborn's degree, while Model (38) can only present the effects of the average degree of newcomers. From the biological point of view, the model based on the log-normal moment assumption will perform better.

3 The Basic Reproduction Number

The basic reproduction number, denoted as R_0, is defined as the average number of secondary infections generated by a single infectious individual introduced into a totally susceptible population during the course of its infectious period[36]. In this section, the basic reproduction numbers of Models (37) and (38) are calculated by analyzing the local stability of the disease-free equilibrium and analyzing the existence of the endemic equilibrium, respectively. As the population size tends to be zero when $b < d$ or infinity when $b > d$, we do not consider these two situations. In what follows, we assume that the population is at equilibrium, which requires $d = b$ and $N(t) \equiv N_0$.

3.1 The Basic Reproduction Number of Model (37)

The basic reproduction number of Model (37) will be derived by analyzing the local asymptotic stability of the disease-free equilibrium.

It is easy to prove that Model (37) always exists a disease-free equilibrium:

$$E_0 = ((1-p)N_0, 0, pN_0, 0, 1-p, \psi'(1), \alpha\psi'(1)),$$

where $\alpha = \frac{\psi''(1)+2\psi'^2(1)}{3\psi'(1)}$. The Jacobian matrix J_0 at E_0 is

$$\begin{pmatrix} -b & 0 & 0 & j_1 & 0 & 0 & 0 \\ 0 & -(b+\gamma) & 0 & j_2 & 0 & 0 & 0 \\ 0 & \gamma & -b & j_3 & 0 & 0 & 0 \\ 0 & \frac{b}{N_0} & 0 & j_4 & 0 & 0 & 0 \\ \frac{b}{N_0} & 0 & 0 & j_5 & -2b & 0 & 0 \\ 0 & 0 & 0 & j_6 & 0 & -2b & 0 \\ -\frac{2b(\psi''(1)-\psi'^2(1))}{3(1-p)N_0} & 0 & 0 & j_7 & 0 & 2b\psi'(1) & -3b \end{pmatrix},$$

where $j_1 = -\lambda(1-p)N_0\psi'(1)$, $j_2 = \lambda(1-p)N_0\psi'(1)$, $j_3 = 0$, $j_4 = \lambda(1-p)\alpha - (\lambda+\gamma+2b)$, $j_5 = -\lambda(1-p)\alpha + \lambda(1-p)$, $j_6 = -\lambda\psi'(1)\,(\alpha+1-\psi'(1))$, $j_7 = -\lambda((\alpha+1)^3 - (\alpha+1)\psi'(1) - \alpha\psi'^2(1))$. Then the characteristic equation is

$$(z+2b)^2(z+3b)(z+b)^2 f(z) = 0, \tag{39}$$

where

$$f(z) = (z+b+\gamma)\,(z - \lambda(1-p)\alpha + \lambda + \gamma + 2b) - \lambda b(1-p)\psi'(1). \tag{40}$$

Thus, all roots of Equation (39) have negative real parts if and only if

$$-(b+\gamma)\,(\lambda(1-p)\alpha - (\lambda+\gamma+2b)) - \lambda b(1-p)\psi'(1) > 0 \tag{41}$$

and

$$-(b+\gamma) + \lambda(1-p)\alpha - (\lambda+\gamma+2b) < 0. \tag{42}$$

Condition (41) implies Condition (42). Hence, Inequality (41) ensures that all eigenvalues of J_0 have negative real parts. Then it follows from (41) that we obtain the basic reproduction number R_0 as follows

$$R_0 = \frac{\lambda(1-p)}{\lambda+\gamma+2b}\left(\alpha + \frac{b\psi'(1)}{b+\gamma}\right). \tag{43}$$

Thus, all eigenvalues of J_0 have negative real parts if $R_0 < 1$, and there is at least one positive eigenvalue if $R_0 > 1$. Therefore, E_0 is locally asymptotically stable if $R_0 < 1$ and unstable if $R_0 > 1$.

Remark 1 If there is no demographic changes, i.e., $b = 0$ and $p = 0$, then

$$R_0 = \frac{\lambda\alpha}{\lambda+\gamma}. \tag{44}$$

Note that $\alpha = \frac{\langle k^2\rangle - \langle k\rangle}{\langle k\rangle}$ when there is no disease in the network, where $\langle k^m\rangle$ is the mth order original moment of the network degree distribution. Therefore, we get the same reproduction number as given by the effective degree model in [15].

Remark 2 If the degree of newcomers is Poisson distributed with parameter ν, then the basic reproduction number is

$$R_0 = \frac{\lambda(1-p)(2b+\gamma)\nu}{(\lambda+\gamma+2b)(b+\gamma)}.$$

If it is scale-free distributed as follows

$$\pi_k = (1+\nu)m^{1+\nu}k^{-2-\nu}, \quad k = m, m+1, \cdots,$$

then,

$$R_0 = \begin{cases} \infty, & \gamma \leqslant 1, \\ \dfrac{\lambda(1-p)}{\lambda+\gamma+2b}\left(\dfrac{\nu m}{3(\nu-1)} + \dfrac{(5b+2\gamma)(1+\nu)m}{3(b+\gamma)\nu} - \dfrac{1}{3}\right), & \gamma > 1, \end{cases}$$

where m is the minimum degree.

Remark 3 Denote V as the variance of newcomers' degrees, then

$$R_0 = \frac{\lambda(1-p)}{\lambda+\gamma+2b}\left(\frac{V+3\psi'^2(1)-\psi'(1)}{3\psi'(1)} + \frac{b\psi'(1)}{b+\gamma}\right). \tag{45}$$

Obviously, R_0 is an increasing function of V. Thus, increasing the variance of newcomer's degree may lead to the epidemic outbreak even if the transmission rate is small.

3.2 The Basic Reproduction Number of Model (38)

The basic reproduction number of Model (38) will be derived by discussing the condition for the existence of endemic equilibrium E^*. The endemic equilibrium is given by setting zeros in the left hand sides of Model (38), and $[I] \neq 0$. Suppose $E^* = (S^*, I^*, R^*, p^*_{si}, p^*_{ss}, g^*_s)$, then it satisfies

$$\begin{cases} S^* = \dfrac{(1-p)bN_0}{b+\lambda p^*_{si} g'^*_s}, & \text{(46a)} \\ I^* = \dfrac{\lambda p^*_{si} g'^*_s}{b+\gamma} S^*, & \text{(46b)} \\ \lambda p^*_{ss}(g'^{*2}_s - g'^*_s) - (\lambda+\gamma)g'^*_s + \lambda p^*_{si} g'^*_s + \dfrac{\lambda b(1-p)}{b+\gamma}\psi'(1)g'^*_s & \\ -\lambda p^*_{si}\psi'(1)g'^*_s - 2b\psi'(1) = 0, & \text{(46c)} \\ -\lambda p^*_{si} p^*_{ss}(g'^{*2}_s - g'^*_s) + \lambda p^*_{si} p^*_{ss} g'^*_s + 2b(1-p)\psi'(1) & \\ -\lambda p^*_{si} p^*_{ss}\psi'(1)g'^*_s - 2b\psi'(1)p^*_{ss} = 0, & \text{(46d)} \\ 2b\psi'(1) - 2bg'^*_s + \lambda p^*_{si} g'^*_s \psi'(1) - \lambda p^*_{si} g'^{*2}_s = 0. & \text{(46e)} \end{cases}$$

Following Equation (46e), it is easy to see that $g'^*_s = \psi'(1)$. Substituting it into Equations (46c) and (46d) yields

$$-\lambda p^*_{si} p^*_{ss}\psi'(1) + \lambda p^*_{si} p^*_{ss} + b(1-p) - bp^*_{ss} = 0 \tag{47}$$

and

$$\lambda p^*_{ss}\psi'(1) - \lambda p^*_{ss} - (\lambda+\gamma) + \lambda p^*_{si} + \frac{\lambda b(1-p)}{d+\gamma}\psi'(1) - \lambda p^*_{si}\psi'(1) - 2b = 0. \tag{48}$$

Then multiplying Equation (47) by p_{ss}, and subtracting Equation (48) gets

$$\lambda(\psi'(1)-1)p_{ss}^{*2}-\left(\lambda+\gamma+b-\frac{\lambda b(1-p)}{d+\gamma}\psi'(1)\right)p_{ss}^{*}-b(1-p)=0. \tag{49}$$

Obviously, Equation (49) has one positive solution and one negative solution, with the positive solution being

$$p_{ss}^{*}=\frac{(\lambda+\gamma+b-\frac{\lambda b(1-p)}{d+\gamma}\psi'(1))+\sqrt{\Delta}}{2\lambda(\psi'(1)-1)}, \tag{50}$$

where

$$\Delta=\left(\lambda+\gamma+b-\frac{\lambda b(1-p)}{d+\gamma}\psi'(1)\right)^{2}+4b(1-p)\lambda(\psi'(1)-1).$$

Substituting (50) into Equation (46d) yields

$$p_{si}^{*}=\frac{b(p_{ss}^{*}+p-1)}{\lambda p_{ss}^{*}(1-\psi'(1))}. \tag{51}$$

Then, we obtain

$$S^{*}=\frac{(1-p)bN_0}{d+\lambda p_{si}^{*}\psi'(1)},\qquad I^{*}=\frac{\lambda(1-p)bN_0p_{si}^{*}\psi'(1)}{(d+\gamma)(d+\lambda p_{si}^{*}\psi'(1))},\qquad R^{*}=N_0-S^{*}-I^{*}.$$

In order to show that E^{*} is an endemic equilibrium, we must prove the condition for the existence of endemic equilibrium, i.e., $0<p_{ss}^{*}<1-p$. Let

$$y(p_{ss})=\lambda(\psi'(1)-1)p_{ss}^{2}-\left(\lambda+\gamma+b-\frac{\lambda b(1-p)}{d+\gamma}\psi'(1)\right)p_{ss}-b(1-p).$$

Then

$$y(1-p)>0,$$

which means

$$\frac{\lambda(1-p)}{\lambda+\gamma+2b}\left(\psi'(1)-1+\frac{b\psi'(1)}{b+\gamma}\right)>1.$$

Denote

$$R_0'=\frac{\lambda(1-p)}{\lambda+\gamma+2b}\left(\psi'(1)-1+\frac{b\psi'(1)}{b+\gamma}\right). \tag{$*$}$$

Hence, Model (38) has a unique endemic equilibrium E^{*} when $R_0'>1$. Here, R_0' is defined as the basic reproduction number of Model (38).

Comparing (*) with (43), there is only one different term in the bracket. Note that they are derived from different assumptions. R_0 is derived under the assumption $E(X^3)=\left(\frac{E(X^2)}{E(X)}\right)^3$, while R_0' is derived under the assumption $E(X^2)=(E(X))^2$. In fact, $\alpha=\frac{\psi''(1)+2\psi'(1)}{3\psi'(1)}$ in R_0 and $\psi'(1)-1$ in R_0' are the values of $\frac{g_s''}{g_s'}$ in the disease-free equilibrium under different assumptions.

3.3 Relationship Between Recruitment Rate and the Basic Reproduction Number

In this section, we will discuss the relationship between recruitment rate and the basic reproduction number of Model (37) in more detail. Because the disease will always die out when $b = 0$, only the situation $b > 0$ is discussed.

Proposition 1 *Considering a simple case in which the degree of newcomers is Poisson distributed and $p = 0$, then $\psi''(1) = \psi'^2(1)$ and*

$$R_0 = \frac{\lambda\psi'(1)(2b+\gamma)}{(\lambda+\gamma+2b)(b+\gamma)}.$$

Hence, there is a complex relationship between the recruitment rate and R_0 as given in Table 2, and this relationship depends on the average degree of newcomers.

Proof Define

$$f(b) = 2b^2 + (\lambda + 3\gamma - 2\lambda\psi'(1))b + \gamma(\lambda + \gamma - \lambda\psi'(1)), \tag{52}$$

then $R_0 > 1$ (or $R_0 < 1$) corresponds to $f(b) < 0$ (or $f(b) > 0$).

Let

$$\begin{aligned} \triangle &= (\lambda + 3\gamma - 2\lambda\psi'(1))^2 - 8\gamma(\lambda + \gamma - \lambda\psi'(1)) \\ &= (2\lambda\psi'(1) - \lambda - \gamma)^2 - 4\lambda\gamma. \end{aligned} \tag{53}$$

Then $f(b) = 0$ has the following two roots

$$b_1^* = \frac{-(\lambda + 3\gamma - 2\lambda\psi'(1)) - \sqrt{\triangle}}{4}, \quad b_2^* = \frac{-(\lambda + 3\gamma - 2\lambda\psi'(1)) + \sqrt{\triangle}}{4}.$$

Next, we discuss (52) in different situations.

(A) If $\frac{\lambda+\gamma-2\sqrt{\lambda\gamma}}{2\lambda} < \psi'(1) < \frac{\lambda+\gamma+2\sqrt{\lambda\gamma}}{2\lambda}$, then $\triangle < 0$. Hence, $f(b) > 0$ for $b > 0$.

(B) If $\psi'(1) = \frac{\lambda+\gamma-2\sqrt{\lambda\gamma}}{2\lambda}$ or $\psi'(1) = \frac{\lambda+\gamma+2\sqrt{\lambda\gamma}}{2\lambda}$, then $\triangle = 0$ and $b_1^* = b_2^*$.

For $\psi'(1) = \frac{\lambda+\gamma-2\sqrt{\lambda\gamma}}{2\lambda}$, it has $b_1^* = -\frac{1}{4}(2\gamma + 2\sqrt{\lambda\gamma}) < 0$. Then $f(b) > 0$ for $b > 0$.

For $\psi'(1) = \frac{\lambda+\gamma+2\sqrt{\lambda\gamma}}{2\lambda}$, it has $b_1^* = -\frac{1}{2}(\gamma - \sqrt{\lambda\gamma})$. Then $b_1^* > 0$ if $\lambda > \gamma$, otherwise $b_1^* \leqslant 0$. Hence, if $\lambda \leqslant \gamma$, then $f(b) > 0$ for $b > 0$. If $\lambda > \gamma$, then $f(b) = 0$ for $b = b_1^*$, and $f(b) > 0$ for $b \in (0, b_1^*) \cup (b_1^*, +\infty)$.

(C) If $|2\lambda\psi'(1) - \lambda - \gamma| > 2\sqrt{\lambda\gamma}$ and $(\lambda + 3\gamma - 2\lambda\psi'(1)) \geqslant \sqrt{\triangle}$, i.e., $\psi'(1) < \frac{\lambda+\gamma-2\sqrt{\lambda\gamma}}{2\lambda}$, or $\frac{\lambda+\gamma+2\sqrt{\lambda\gamma}}{2\lambda} < \psi'(1) \leqslant \frac{\lambda+\gamma}{\lambda}$ and $\lambda \leqslant \gamma$, then $\triangle > 0$ and $b_2^* \leqslant 0$. Hence, one has $f(b) > 0$ for $b > 0$.

(D) If $\psi'(1) \geqslant \frac{\lambda+\gamma}{\lambda}$, then $\triangle > 0$, $b_1^* \leqslant 0$ and $b_2^* > 0$. Hence, one has $f(b) < 0$ for $b \in (0, b_2^*)$ and $f(b) > 0$ for $b \in (b_2^*, +\infty)$.

(E) If $\frac{\lambda+\gamma+2\sqrt{\lambda\gamma}}{2\lambda} < \psi'(1) < \frac{\lambda+\gamma}{\lambda}$ and $\lambda > \gamma$, then $\triangle > 0$ and $b_1^* > 0$. Hence, one has $f(b) < 0$ for $b \in (b_1^*, b_2^*)$ and $f(b) > 0$ for $b \in (0, b_1^*) \cup (b_2^*, +\infty)$.

In conclusion, the relationship between recruitment rate and R_0 given λ and γ is summarized as in Table 2. ∎

Table 2 Relationship between the recruitment rate and R_0

$\lambda \leqslant \gamma$	$\psi'(1) \leqslant \frac{\lambda+\gamma}{\lambda}$	$b \in (0, +\infty)$	$R_0 < 1$
	$\psi'(1) > \frac{\lambda+\gamma}{\lambda}$	$b < b_2^*$	$R_0 > 1$
		$b = b_2^*$	$R_0 = 1$
		$b > b_2^*$	$R_0 < 1$
$\lambda > \gamma$	$\psi'(1) < \frac{2\sqrt{\lambda\gamma}+\lambda+\gamma}{2\lambda}$	$b \in (0, +\infty)$	$R_0 < 1$
	$\psi'(1) = \frac{2\sqrt{\lambda\gamma}+\lambda+\gamma}{2\lambda}$	$b \in (0, +b_2^*) \cup (b_2^*, +\infty)$	$R_0 < 1$
		$b = b_2^*$	$R_0 = 1$
	$\frac{2\sqrt{\lambda\gamma}+\lambda+\gamma}{2\lambda} < \psi'(1) < \frac{\lambda+\gamma}{\lambda}$	$b_1^* < b < b_2^*$	$R_0 > 1$
		$b \in \{b_1^*, b_2^*\}$	$R_0 = 1$
		$b \in (0, b_1^*) \cup (b_2^*, +\infty)$	$R_0 < 1$
	$\psi'(1) \geqslant \frac{\lambda+\gamma}{\lambda}$	$b < b_2^*$	$R_0 > 1$
		$b = b_2^*$	$R_0 = 1$
		$b > b_2^*$	$R_0 < 1$

Figure 3 describes three special cases. It reflects that increasing the recruitment rate may lead to the change of R_0 from $R_0 > 1$ to $R_0 < 1$. As a larger recruitment rate means a larger death rate, it effectively decreases the number of infectious individuals in the population which further inhibits the spread of disease. From Figure 3(a), it is observed that a larger recruitment may change R_0 from $R_0 < 1$ to $R_0 > 1$ when $\lambda > \gamma$ and $\psi'(1) \in (\frac{2\sqrt{\lambda\gamma}+\lambda+\gamma}{2\lambda}, \frac{\lambda+\gamma}{\lambda})$. It is due to the fact that with the increase of recruitment rate, more susceptible individuals enter into the population which contribute to accelerate the spread of disease. In addition, it is worth noting that $\frac{\lambda+\gamma}{\lambda}$ is the threshold that determines whether a disease can spread throughout the network without demographic process. Thus, the recruitment and death of population can lead to the outbreak of epidemics.

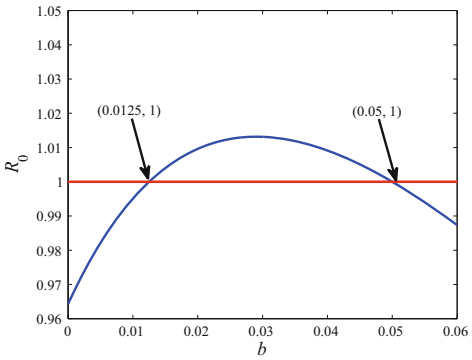

(a) $\lambda = 0.25$, $\psi'(1) = 1.35$

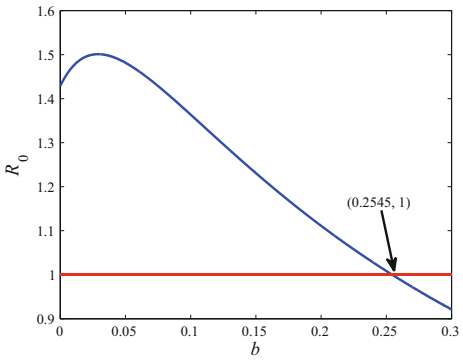

(b) $\lambda = 0.25$, $\psi'(1) = 2$

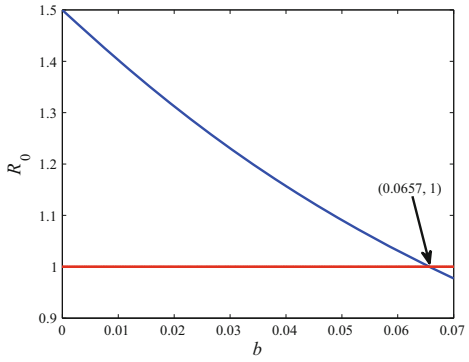

(c) $\lambda = 0.02$, $\psi'(1) = 10$

Figure 3 Relationship between recruitment rate (b) and the basic reproduction number (R_0) with parameters: $d = b$, $p = 0$, $\gamma = 0.1$, $\psi''(1) = \psi'^2(1)$, $I(0) = 5$, $N(0) = 1000$

4 Simulation Results

In this section, a series of stochastic and numerical simulations are performed to validate the theoretical results.

First, stochastic simulations of SIR epidemic model with demographics are performed to compare with the numerical results of the ODE models. The stochastic simulation process starts from a network with $N(0)$ nodes, in which $I(0)$ randomly selected nodes are set to be infectious, and the remaining nodes are set to be susceptible. Then the epidemic process and demographic process are considered simultaneously in every time step Δt. For the epidemic process, each node updates its disease state, i.e., nodes in susceptible state are infected with probability $\lambda n \Delta t$, where n is the number of infectious neighbors, and nodes in infectious state recover with probability $\gamma \Delta t$. For the demographic process, we extract two random numbers, $B(t)$ and $D(t)$, from a binomial distribution $Bino(N(t), b\Delta t)$. Then $D(t)$ randomly selected nodes, together with their links, are removed from the network. $B(t)$ new nodes connect to existing nodes randomly, and the number of links each new node emits is extracted from the distribution π_k. The epidemic and demographic process repeat until the epidemic dies out or the given simulation time is reached. Finally, the process is repeated 50 times independently, and each time series of the prevalence is recorded.

Based on the above ideas, we perform the stochastic simulations. Figure 4 provides the comparison between the numerical results of the ODE models and mean values of stochastic simulations. It is clear to see that the zero variance assumption can only perform as well as the log-normal moment closure assumption when the variance of newcomer's degree is smaller. Furthermore, the log-normal moment closure assumption performs better when the variance of newcomer's degree is larger. This is due to that newcomers contact existing nodes in network randomly. A larger variance of newcomer's degree will cause a larger variance of susceptible nodes' degrees, which leads to considerable errors when we simply assume the variance as zero. More importantly, Model (37) closely captures the exponential growth rate and equilibrium

point of epidemic. So it is more rational to use the log-normal moment closure assumption to truncate the epidemic model. Excellent agreements between the numerical results of Model (37) and the mean values of stochastic realizations indicate that Model (37) can be used as an effective tool to investigate the dynamics of epidemic with demographics.

In Figure 5, we plot the final density of infectious nodes ($[I]^*/N$) between the mean ($\psi'(1)$) and variance (V) of newcomers' degrees. Figures 5(a)–5(b) indicate that increasing the variance of newcomer's degree may promote the disease spread throughout the population when the transmission rate is small. This is because that a larger variance of newcomer's degree increases the heterogeneity of network, which facilitates the spread of epidemic. This finding is consistent with the analysis of R_0, in which a sufficient large variance of newborn's degree will lead to $R_0 > 1$ when the transmission rate is small. However, a larger variance of newcomers' degrees contributes to a slight decrease of the final density of infectious nodes when the transmission rate is large. For a larger transmission, a lot of infection is presented. And for a given average degree of newcomers, if the variance is high, more low degree nodes are born. The "average" node is likely infected quickly, but there are many nodes which are well above or below the average. The nodes above average get infected quickly, but that is not really different from the average nodes. The nodes below average get infected more slowly, explaining the network effect. This is similar to the observation that higher variance in degree tends to cause smaller epidemics in static networks. As seen from Figure 1 in [8], with the same mean degree in the case of large transmission rate, the density of infected nodes in the BA network is smaller than the one in the WS network.

Figure 6 shows the influence of the recruitment rate on the final density of infectious nodes, where the row coordinates of red dots are calculated from $R_0 = 1$. Obviously, at lower b, nodes tend to recover before dying, so it does not affect further transmission significantly. However, at larger b, nodes tend to die before recovering. Large b means that infectious nodes tend to die before transmitting. In conclusion, higher birth rate tends to stop the disease. Besides, Figure 6 verifies the results of Subsection 3.3 where the disease will disappear in the population if $R_0 < 1$, and it will spread throughout the population if $R_0 > 1$.

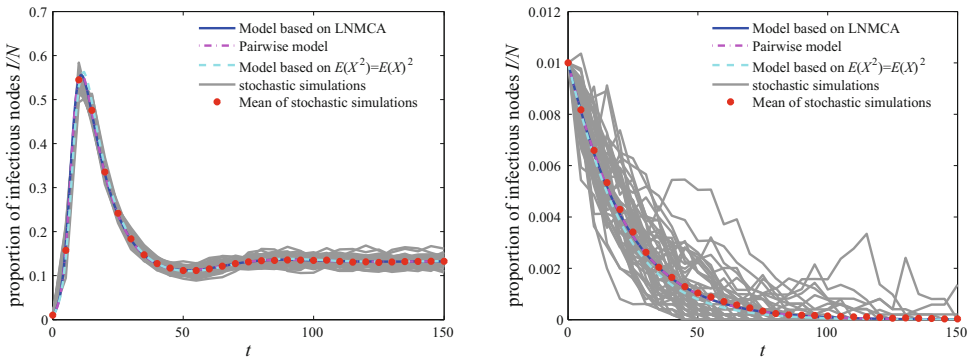

(a) $R_0 = 4.2424$ (b) $R_0 = 0.6306$

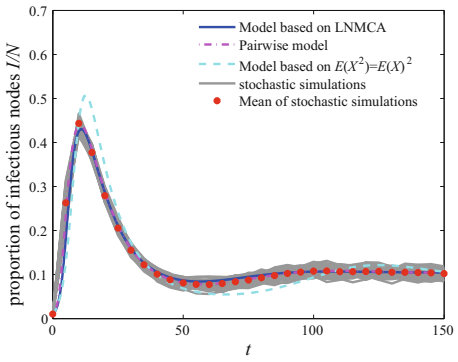

(c) $R_0 = 3.1819$

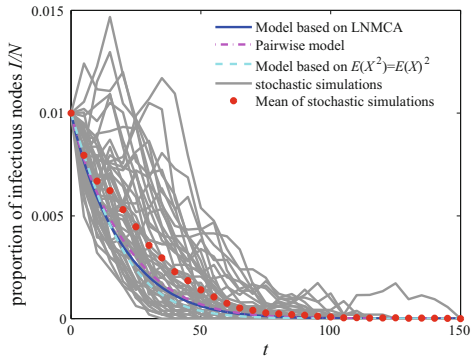

(d) $R_0 = 0.4730$

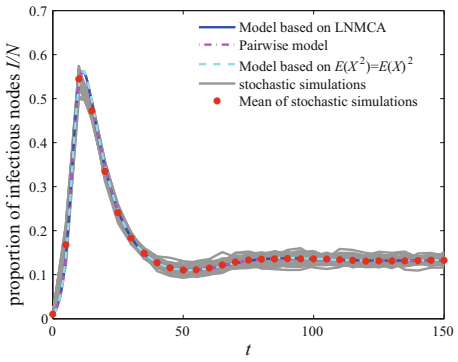

(e) $R_0 = 4.1212$

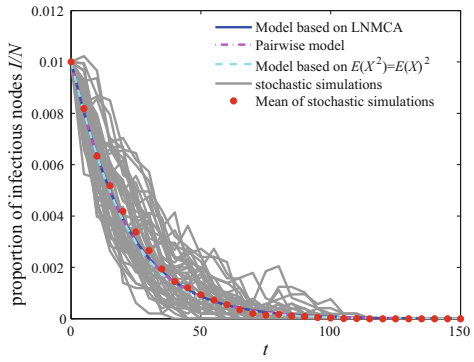

(f) $R_0 = 0.6126$

Figure 4 Comparison between the mean values of stochastic simulations and numerical simulations for dynamics of fraction of infectious individuals with different degree distribution of newcomers. In these simulations, the parameters are $\gamma = 0.1$, $b = 0.02$, $I(0) = 50$, $N(0) = 5000$, and $\lambda = 0.08$ ((a), (c) and (e)), $\lambda = 0.008$ ((b), (d) and (f)). In (a) and (b), the degree of newcomers are Poisson distributed with $\pi_k = \frac{\psi'(1)^k}{k!}\mathrm{e}^{-\psi'(1)}$, where $\psi'(1) = 10$. Then $\psi''(1) = 100$. In (c) and (d), the degree of newcomers are distributed as $\pi_k = \frac{k^{-2.7}}{\sum_{k=3}^{k=100} k^{-2.7}}, k = 3, 4, \cdots, 100$. Then $\psi'(1) = 5.7419$, $\psi''(1) = 68.3068$. In (e) and (f), newcomers have the same degree 10, i.e., $\pi_{10} = 1$, and $\pi_k = 0$ for $k \neq 10$. Then $\psi'(1) = 10$, $\psi''(1) = 90$

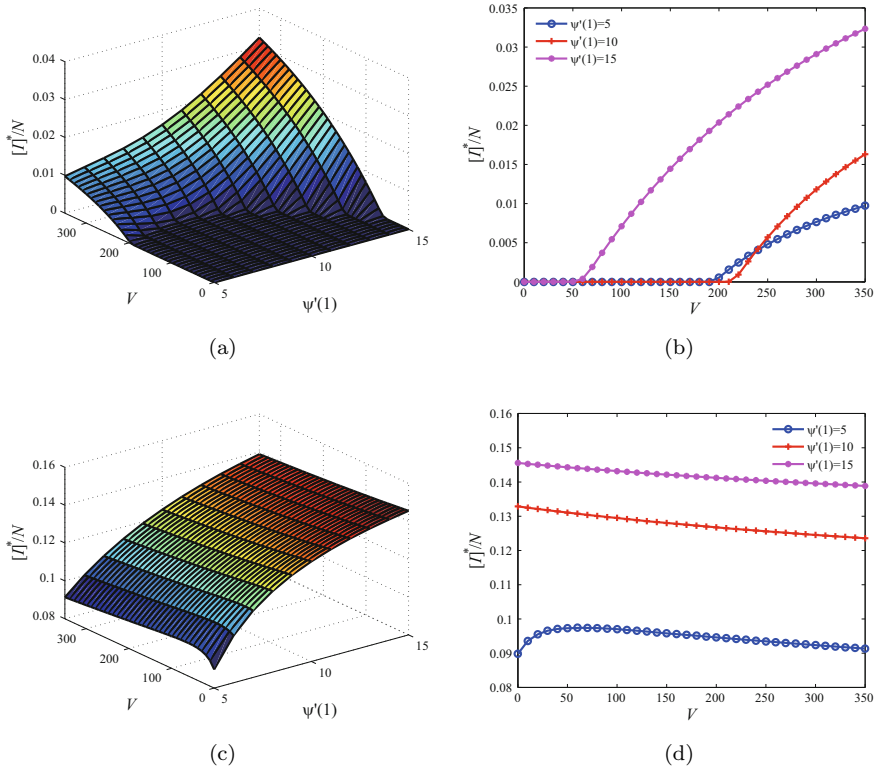

Figure 5 The effect of the mean ($\psi'(1)$) and variance (V) of newcomers' degrees on the final density of infectious nodes ($\frac{[I]^*}{N}$). The parameter values are: $p = 0, b = 0.02, d = b$, $\gamma = 0.1$, and $\lambda = 0.008$ ((a) and (b)), $\lambda = 0.08$ ((c) and (d))

Finally, Figure 7 indicates that vaccination of newcomers is an effective method to control the spread of epidemics.

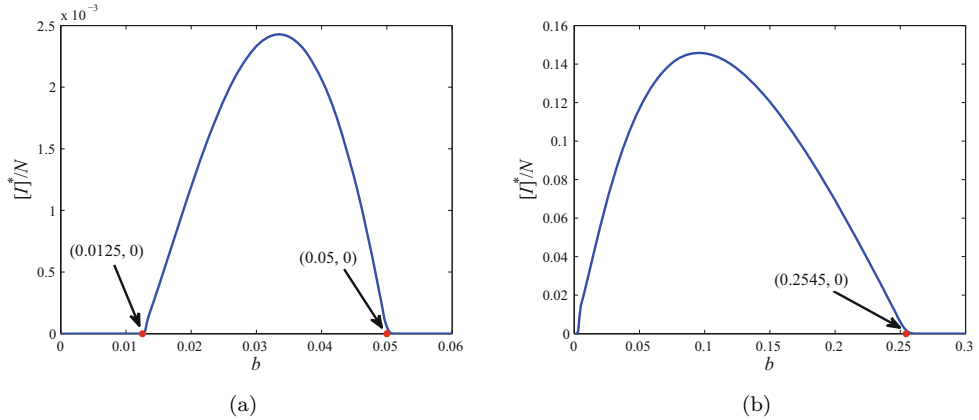

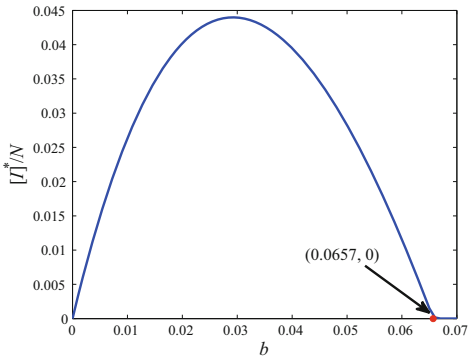

(c)

Figure 6 Relationships between recruitment rate (b) and final densities of infectious nodes ($\frac{[I]^*}{N}$) with parameters: $d = b$, $\gamma = 0.1$, $p = 0$, $\psi''(1) = \psi'^2(1)$, $I(0) = 5$, $N(0) = 1000$ and (a) $\lambda = 0.25$, $\psi'(1) = 1.35$, (b) $\lambda = 0.25$, $\psi'(1) = 2$; (c) $\lambda = 0.02$, $\psi'(1) = 10$

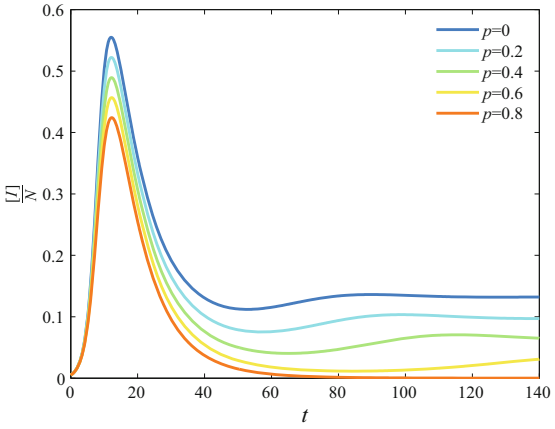

Figure 7 The effect of vaccination on the density of infectious nodes with parameters $d = b = 0.02$, $\lambda = 0.08$, $\gamma = 0.1$, $\psi'(1) = 5$

5 Conclusions

For diseases with a long course such that the individuals' connectivity pattern varies on a time scale comparable to that of the epidemic spreading process, new born nodes join the network and meanwhile dead nodes leave the network during the epidemic. This demographic process changes the network structure, which in turn affects the spread of disease. Hence, it is important to incorporate the demographic process into an epidemic model. Based on this consideration, an SIR pairwise epidemic model with demographics is established. This model is further expressed with another form depending on the moments of the susceptible degree distribution. Then the log-normal moment closure and zero variance assumptions are adopted

to obtain two low-dimensional Models (37) and (38), respectively. Furthermore, we derive the basic reproduction number of Model (37) by analyzing the local stability of the disease-free equilibrium, and derive the basic reproduction number of Model (38) by analyzing the existence of the endemic equilibrium. Comparisons between numerical and stochastic simulations show that the zero variance assumption can perform as well as the log-normal moment assumption when the variance of newcomers' degrees is small. The log-normal moment assumption performs better even if the variance of newborns' degrees is large. More importantly, the low-dimensional model based on log-normal assumption closely captures the dynamic properties of disease. So Model (37) is a good approximation to the stochastic SIR process. Numerical simulation of Model (37) shows that increasing the variance of newcomers' degrees may promote the disease spread throughout the population when the transmission rate is small. It contributes to a slight decrease of the final density of infectious nodes when the transmission rate is large. Besides, it is discovered that a large recruitment may hinder the spread of disease.

However, it is assumed that newcomers randomly contact existing nodes in this process. In fact, newcomers may adjust their behaviors according to the epidemic prevalence. For example, they may reduce their contacts during epidemic period and recover these contacts after the epidemic. In this situation, the degree distribution of new nodes may vary with the density of infectious nodes. Furthermore, newcomers may avoid to contact with infectious nodes. It is of interest to study the dynamic behaviors in this project. In addition, two friends of a person are more likely to be friends in real society. Similarly, a new node will link an existing node with higher probability if it has already made a link to one of its neighbors. This evolution mechanism will construct a network with clusters, which is worth to study in future.

References

[1] Anderson R M, Jackson H C, May R M, et al., Population dynamics of fox rabies in Europe, *Nature*, 1981, **289**(5800): 765–771.

[2] Zhang J, Jin Z, Sun G, et al., Analysis of rabies in China: Transmission dynamics and control, *PLoS One*, 2011, **6**(7): e20891.

[3] Zhang J, Jin Z, Sun G, et al., Determination of original infection source of H7N9 avian influenza by dynamical model, *Scientific Reports*, 2014, **4**(6183): 4846.

[4] Ling M, Sun G, Wu Y, et al., Transmission dynamics of a multi-group brucellosis model with mixed cross infection in public farm, *Applied Mathematics and Computation*, 2014, **237**(5): 582–594.

[5] Ling M, Jin Z, Sun G, et al., Modeling direct and indirect disease transmission using multi-group model, *Journal of Mathematical Analysis and Applications*, 2017, **446**(2): 1292–1309.

[6] Pastor-Satorras R and Vespignani A, Epidemic spreading in scale-free networks, *Physical Review Letters*, 2001, **86**(14): 3200–3203.

[7] Newman M E J, Strogatz S H, and Watts D J, Random graphs with arbitrary degree distributions and their applications, *Physical Review E*, 2001, **64**(2): 026118.

[8] Pastor-Satorras R and Vespignani A, Epidemic dynamics and endemic states in complex networks, *Physical Review E*, 2001, **63**(6): 066117.

[9] May R M and Lloyd A L, Infection dynamics on scale-free networks, *Physical Review E*, 2001, **64**(6): 066112.

[10] House T and Keeling M J, Insights from unifying modern approximations to infections on networks, *Journal of the Royal Society Interface*, 2011, **8**(54): 67–73.

[11] Miller J C, Spread of infectious disease through clustered populations, *Journal of the Royal Society Interface*, 2009, **6**(41): 1121–1134.

[12] Molina C and Stone L, Modelling the spread of diseases in clustered networks, *Journal of Theoretical Biology*, 2012, **315**: 110–118.

[13] Volz E M, Dynamics of infectious disease in clustered networks with arbitrary degree distributions, Eprint Arxiv, 2010.

[14] Miller J C, Percolation and epidemics in random clustered networks, *Physical Review E*, 2009, **80**(2): 020901.

[15] Lindquist J, Ma J, van den Driessche P, et al., Effective degree network disease models, *Journal of Mathematical Biology*, 2011, **62**(2): 143–164.

[16] Volz E M, SIR dynamics in random networks with heterogeneous connectivity, *Journal of Mathematical Biology*, 2008, **56**(3): 293–310.

[17] Volz E M and Meyers L A, Susceptible-infected-recovered epidemics in dynamic contact networks, *Proceedings of the Royal Society*, 2007, **274**(1628): 2925–2933.

[18] Miller J C, A note on a paper by Erik Volz: SIR dynamics in random networks, *Journal of Mathematical Biology*, 2011, **62**(3): 349–358.

[19] Kamp C, Untangling the interplay between epidemic spread and transmission network dynamics, *PLoS Computational Biology*, 2010, **6**(11): e1000984.

[20] Kamp C, Demographic and behavioural change during epidemics, *Procedia Computer Science*, 2010, **1**(1): 2253–2259.

[21] Jin Z, Sun G, and Zhu H, Epidemic models for complex networks with demographics, *Mathematical Biosciences and Engineering*, 2014, **11**(6): 1295–1317.

[22] Piccardi C, Colombo A, and Casagrandi R, Connectivity interplays with age in shaping contagion over networks with vital dynamics, *Physical Review E*, 2015, **91**(2): 022809.

[23] Erdös P and Rényi A, On random graphs I, *Publicationes Mathematicae*, 1959, **6**: 290–297.

[24] Eames K T D and Keeling M J, Modeling dynamic and network heterogeneities in the spread of sexually transmitted diseases, *Proceedings of the National Academy of Sciences of the United States of America*, 2002, **99**(20): 13330–13335.

[25] Simon P L and Kiss I Z, Super compact pairwise model for SIS epidemic on heterogeneous networks, *Journal of Complex Networks*, 2016, **4**(2): 187–200.

[26] Bauch C T, The spread of infectious diseases in spatially structured populations: An invasory pair approximation, *Mathematical Biosciences*, 2005, **198**(2): 217–237.

[27] Trapman P, Reproduction numbers for epidemics on networks using pair approximation, *Mathematical Biosciences*, 2007, **210**(2): 464–489.

[28] Keeling M J, Multiplicative moments and measures of persistence in ecology, *Journal of Theoretical Biology*, 2000, **205**(2): 269–281.

[29] Ekanayake A J and Allen L J S, Comparison of markov chain and stochastic differential equation population models under higher-order moment closure approximations, *Stochastic Analysis and Applications*, 2010, **28**(6): 907–927.

[30] Miller J C and Kiss I Z, Epidemic spread in networks: Existing methods and current challenges, *Mathematical Modelling of Natural Phenomena*, 2014, **9**(2): 4–42.

[31] Nåsell I, An extension of the moment closure method, *Theoretical Population Biology*, 2003, **64**(2): 233–239.

[32] Whittle P, On the use of the normal approximation in the treatment of stochastic processes, *Journal of the Royal Statistical Society*, 1957, **19**(2): 268–281.

[33] Goutsias J and Jenkinson G, Markovian dynamics on complex reaction networks, *Physics Reports*, 2013, **529**(2): 199–264.

[34] Hiebeler D, Moment equations and dynamics of a household SIS epidemiological model, *Bulletin of Mathematical Biology*, 2006, **68**(6): 1315–1333.

[35] Krishnarajah I, Cook A, Marion G, et al., Novel moment closure approximations in stochastic epidemics, *Bulletin of Mathematical Biology*, 2005, **67**(4): 855–873.

[36] Anderson R M and May R M, *Infectious Diseases of Humans*, Oxford Science, Oxford, 1991.